Electronic Supplementary Material (ESI) for Energy & Environmental Science
This journal is © The Royal Society of Chemistry 2013

Supplementary Information

Interfaces Between Water Splitting Catalysts and Buried Silicon Junctions

Casandra R.Cox,[a] Mark T. Winkler,[b] Joep J. H. Pijpers,[a] Tonio Buonassisi[b,]* and Daniel G. Nocera[a,]*

[a]*Department of Chemistry and* [b]*Department of Mechanical Engineering, Massachusetts Institute of Technology, Cambridge, Massachusetts 02139-4307, United States*

nocera@mit.edu, buonassisi@mit.edu

Index *Page*

Experimental Methods and Table S1 of sheet resistance values S2
Fig. S1. i-V curve for *npp*⁺Si solar cell S3
Fig. S2. SEM images for NiB_i functionalized solar cell S4
Fig. S3. SEM images for NiFeO functionalized solar cell S5
Fig. S4. CV curves of npp^+–Si | N i | CoB_i S6
Fig. S5. CV curves of npp^+–Si | F T O | NiB_i S7
Fig. S6. CV curves of npp^+–Si | N i | NiB_i S8
Fig. S7. CV curves of npp^+–Si | F T O | NiFeO S9
Fig. S8. CV curves of npp^+–Si | N i | NiFeO S10
Fig. S9. Faradaic efficiency measurements for NiB_i functionalize electrodes S11
Fig. S10. Faradaic efficiency measurement for npp^+–Si | N i | NiFeO S12
Fig. S11. Tafel plots for NiB_i functionalized electrodes S13
Fig. S12. Tafel plots for NiFeO functionalized electrodes S14

This journal is © The Royal Society of Chemistry 2013

Experimental Methods

Below, we provide some additional process details on solar cell fabrication, omitted from the main text for conciseness:

Phosphorus diffusion: Prior to P–diffusion, wafers (doped p–type with B; resistivity in the range 2–6 Ω • cm were cleaned using the so-called "RCA" process to remove organic and metallic contaminants as described in the *Handbook of Semiconductor Wafer Cleaning Technology*, W. Kern (Noyes, Park Ridge, 1993). Emitter formation was carried out via phosphorous diffusion in a Tystar 8" $POCl_3$ tube furnace; wafers are loaded into the preheated furnace (550 °C). The temperature is stabilized at 550 °C for 10 min and then ramped to 822 °C at a rate of 8 °C / min. N_2 process gas, bubbled through liquid phosphorus oxychloride, flows past the samples for 20 min; after exposure to the process gas, the samples are held at 822 °C for 20 min. The temperature is then ramped down to 550 °C at about 8 °C / min and the samples are removed to room temperature. This processing yields an emitter with a measured sheet resistivity between 60–70 Ω/sq.

Si_3N_4 layer formation: After etching the PO_x glass as described in the text, wafers were cleaned of organic and metallic contaminants as described above and immediately transferred to a Tystar furnace for low-pressure chemical-vapor deposition. The Si_3N_4 layer was formed by flowing a 3:1 mixture of ammonia and dicholorsilane (pressure = 250 mTorr) at 770 °C for 20 min, yielding an 80 nm–thick film with an index of 2.01. The film is grown slightly thicker than required to accommodate some etching that occurs during subsequent processing.

***p^+* layer formation:** The Si_3N_4 layer was removed from the p–side of silicon wafer using a reactive ion etch (etch chemistry: a mixture of 6:2:1 CHF_3:CF_4:Ar gases at a process pressure of 150 mTorr and 22.5 sccm total flow rate was used in a Southbay RIE at 100 W power dissipation). 1 µm of Al was deposited as described in the text and annealed at 900 °C for 300 s in an environment of flowing N_2 gas (using a Modular Process Technology RTP-600xp). The peak doping level in the silicon and the thickness of the p^+ region is set by solidus line of the binary phase diagram (see, e.g., J. L. Murray, *Bull. At. Phase Diag.,* 1984, **5,** 74–84). At 900 °C, Al is soluble in silicon at approximately 0.007%, or approximately 3.5×10^{18} cm^{-3}, forming a highly conductive silicon phase and facilitating Ohmic contact.

Table S1. Sheet resistance of protective layers

Protective layer	*Sheet resistance (Ω/sq)*
ITO	170
FTO	41
Ni	13

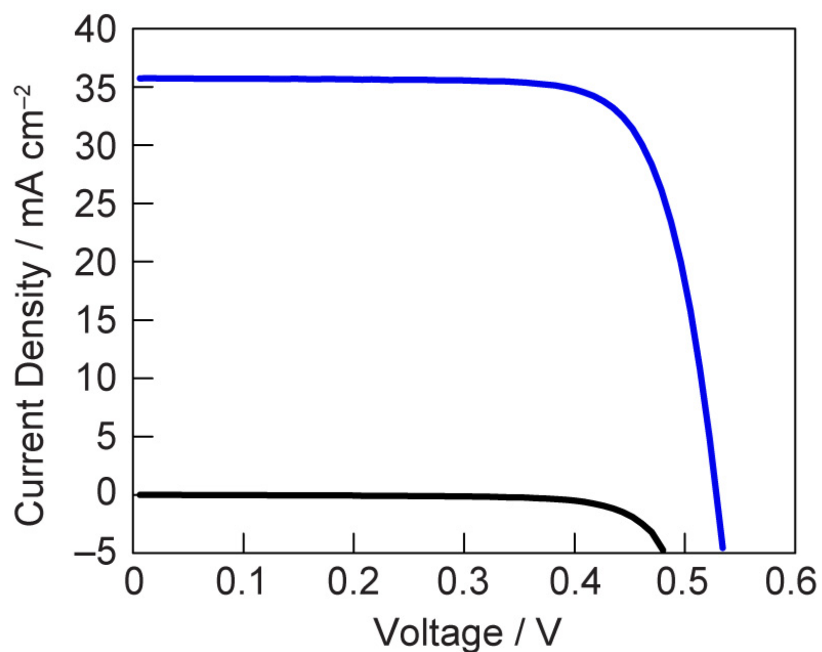

Fig. S1. Representative I-V curve for the *npp*+–Si solar cell used in this study in the dark (▬▬, black) and under AM 1.5 illumination (▬▬, blue). Solar cell properties are: I_{sc} = 35.18 mA/cm², V_{oc} = 0.528 V, FF = 0.76, cell efficiency = 13.22%

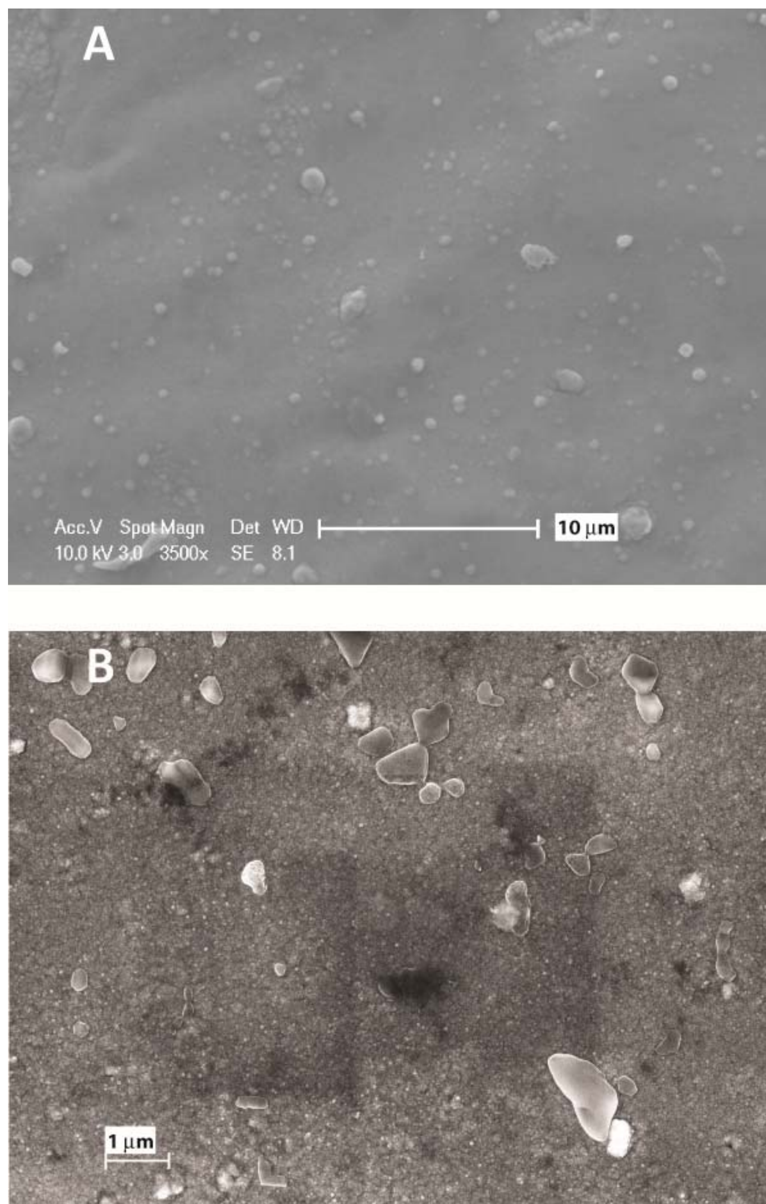

Fig. S2. SEM images of the NiB_i OER–catalysts deposited on surface protected *npp*$^+$–Si electrodes. From left to right (A) *npp*$^+$–Si | FTO | NiB_i, (B) *npp*$^+$–Si | Ni | NiB_i

Electronic Supplementary Material (ESI) for Energy & Environmental Science
This journal is © The Royal Society of Chemistry 2013

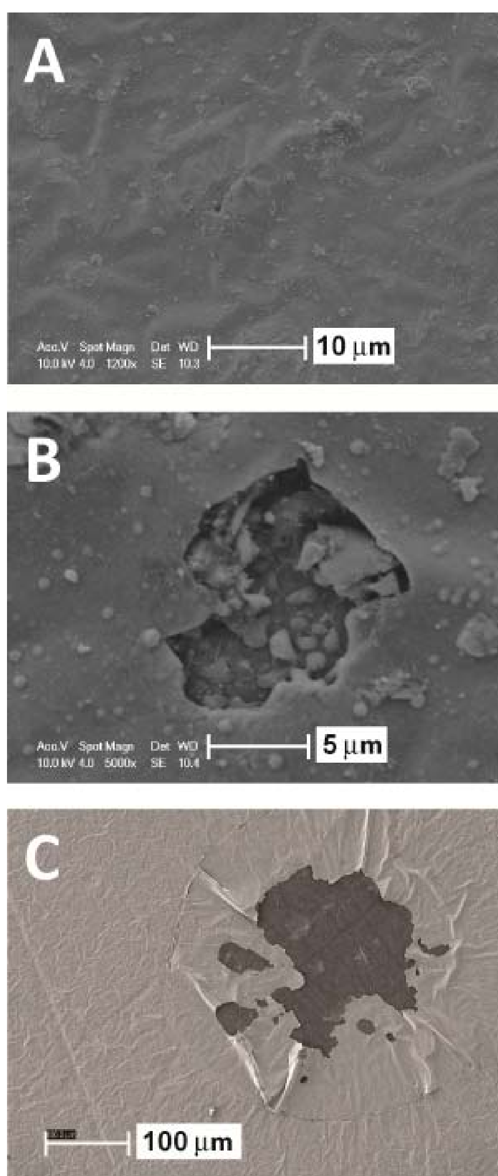

Fig. S3. SEM images of the NiFeO OER–catalysts deposited on surface protected *npp*$^+$–Si electrodes. From left to right (A,B) *npp*$^+$–Si | FTO | NiB_i, (C) *npp*$^+$–Si | Ni | NiB_i

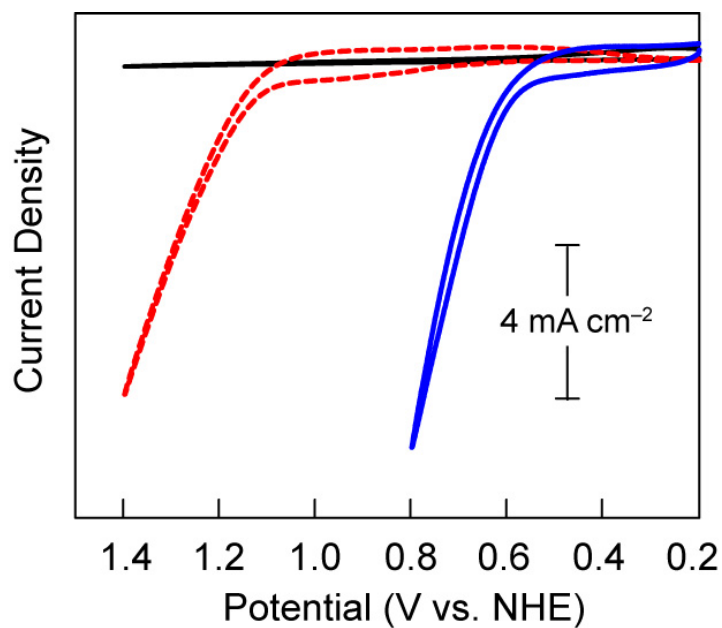

Fig. S4. CV curves of *npp*$^+$–Si | Ni | CoB_i in a 0.5 M KB_i electrolyte in the dark with V_{appl} through the *n*–side of the cell (black solid line), in the dark with V_{appl} through the Ni layer (red dashed line) and under 1 sun AM 1.5 illumination (blue solid line).

Electronic Supplementary Material (ESI) for Energy & Environmental Science
This journal is © The Royal Society of Chemistry 2013

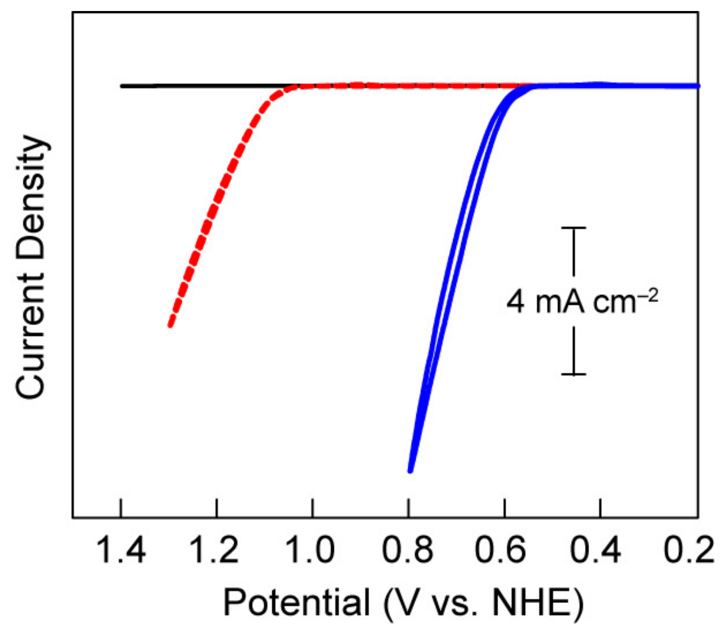

Fig. S5. CV curves of *npp*$^+$–Si | FTO| NiB_i in a 0.5 M KB_i electrolyte in the dark with V_{appl} through the *n*–side of the cell (black solid line), in the dark with V_{appl} through the FTO layer (red dashed line) and under 1 sun AM 1.5 illumination (blue solid line).

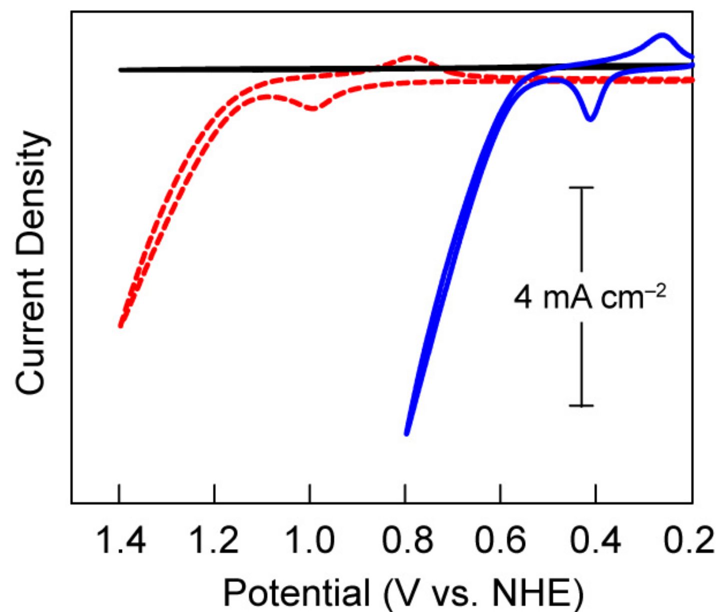

Fig. S6. CV curves of *npp*$^+$–Si | Ni | NiB_i in a 0.5 M KB_i electrolyte in the dark with V_{appl} through the *n*–side of the cell (black solid line), in the dark with V_{appl} through the Ni layer (red dashed line) and under 1 sun AM 1.5 illumination (blue solid line).

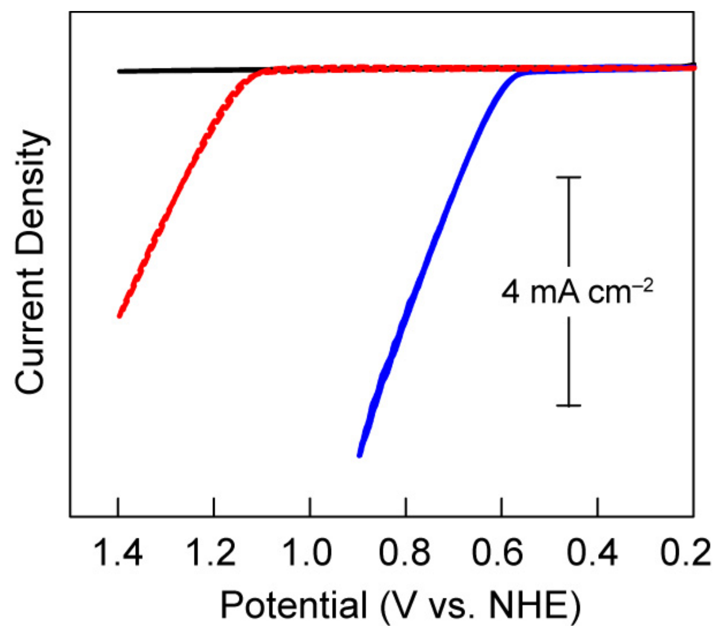

Fig. S7. CV curves of *npp*+–Si | FTO | NiFeO in a 0.5 M KB_i electrolyte in the dark with V_{appl} through the *n*–side of the cell (black solid line), in the dark with V_{appl} through the FTO layer (red dashed line) and under 1 sun AM 1.5 illumination (blue solid line).

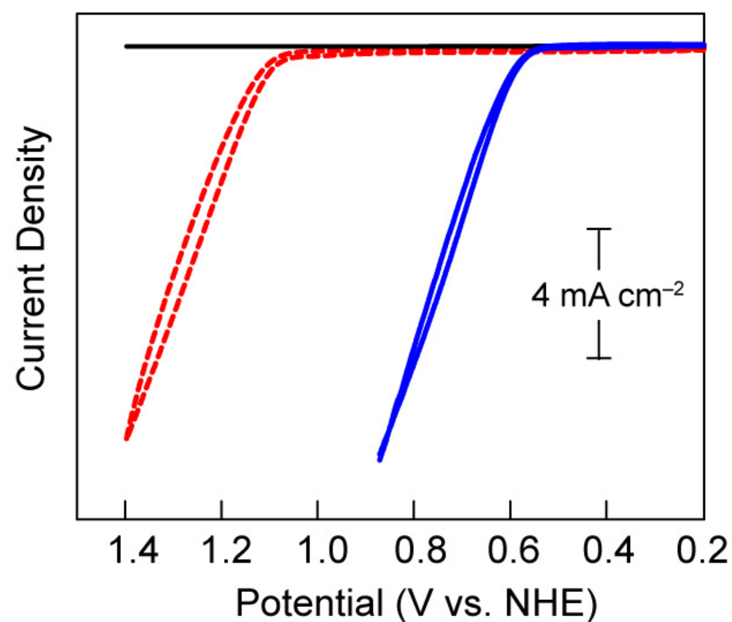

Fig. S8. CV curves of *npp*⁺–Si | Ni | NiFeO in a 0.5 M KB_i electrolyte in the dark with V_{appl} through the *n*–side of the cell (black solid line), in the dark with V_{appl} through the Ni layer (red dashed line) and under 1 sun AM 1.5 illumination (blue solid line).

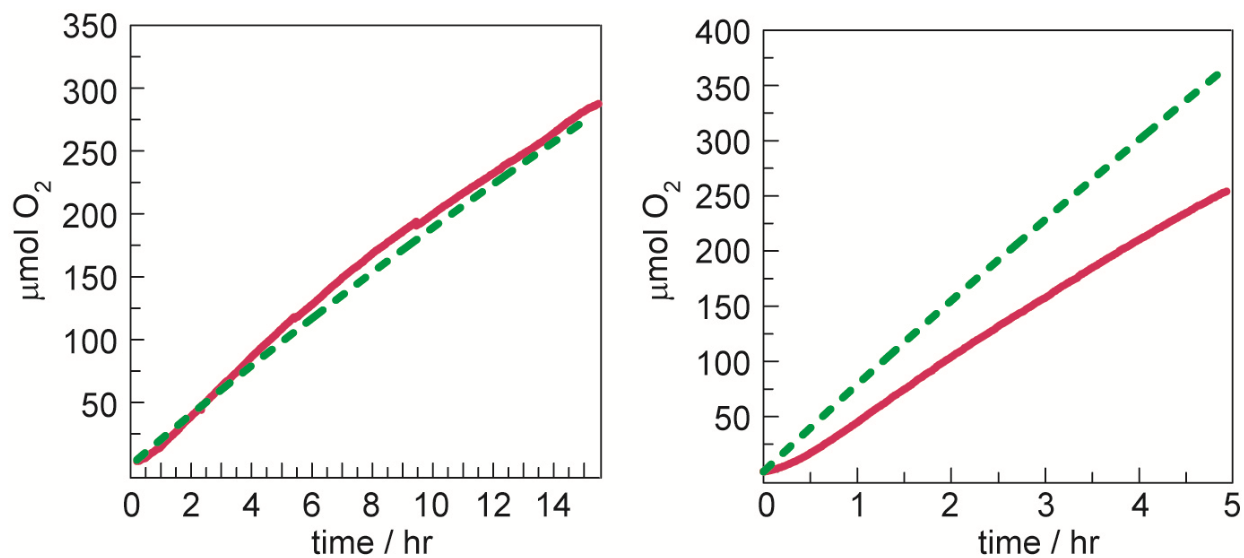

Fig. S9. O_2 production measured by a fluorescent sensor (red solid line) and the amount produced based on current passed assuming 100% Faradaic efficiency (green dashed line) for (left) *npp*$^+$–Si | FTO | NiB_i and (right) *npp*$^+$–Si | Ni | NiB_i.

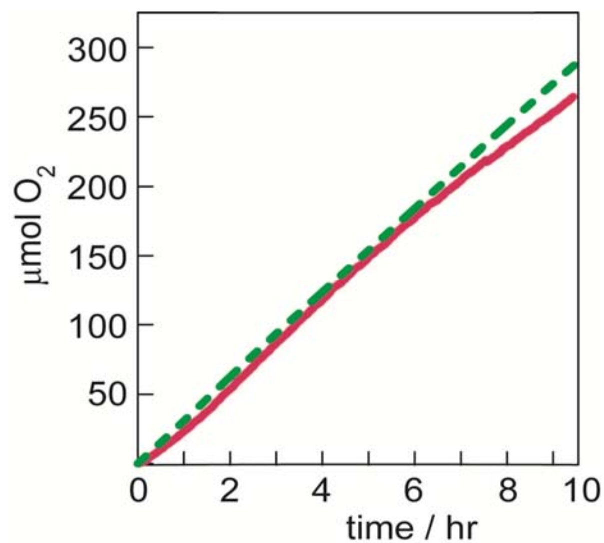

Fig. S10. O_2 production for *npp*+–Si | Ni | NiFeO measured by a fluorescent sensor (red solid line) and the theoretical amount of produced O_2 (green dashed line), obtained from the I-t curve, assuming a Faradaic efficiency of 100%.

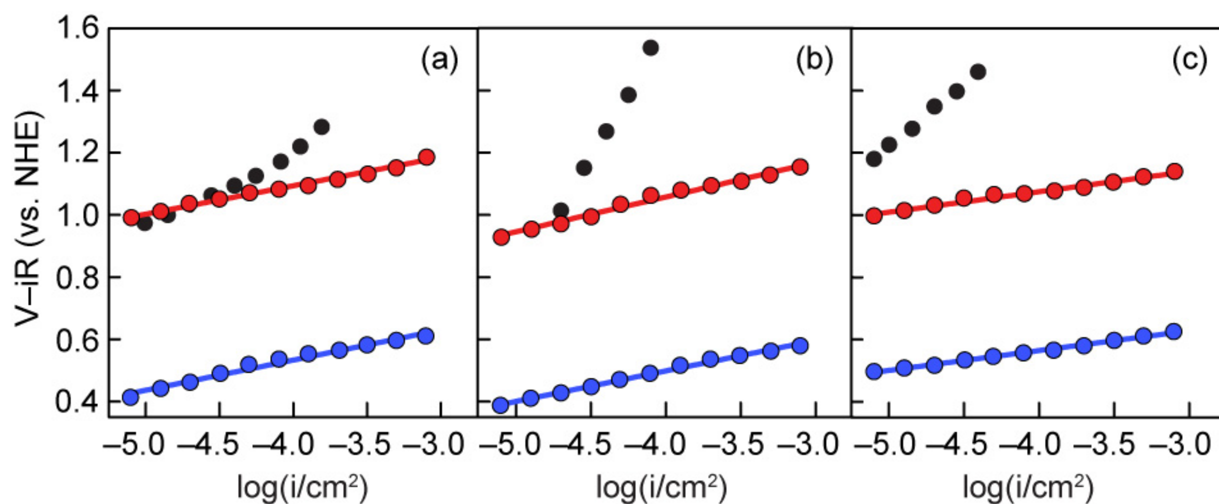

Fig. S11. Tafel plots from of (a) *npp*$^+$–Si | ITO | NiB$_i$, (b) *npp*$^+$–Si | FTO | NiB$_i$ and (c) *npp*$^+$–Si | Ni | NiB$_i$. With the potential applied to the metal front contact for measurements in the dark (black), under 1 sun of AM 1.5 illumination (blue), and in the dark with the potential applied through the protective coating at the back of the sample (red).

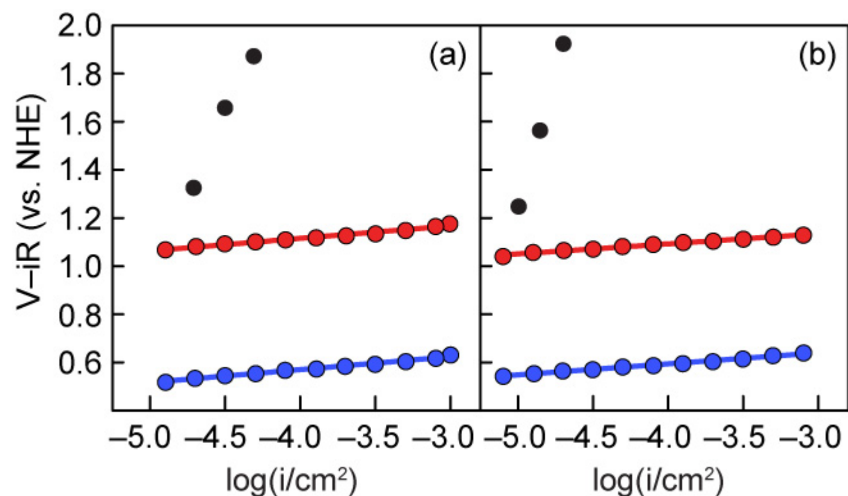

Fig. S12. Tafel plots from of (a) *npp*+–Si | FTO| NiFeO, (b) *npp*+–Si | Ni | NiFeO .With the potential applied to the metal front contact for measurements in the dark (black), under 1 sun of AM 1.5 illumination (blue), and in the dark with the potential applied through the protective coating at the back of the sample (red).